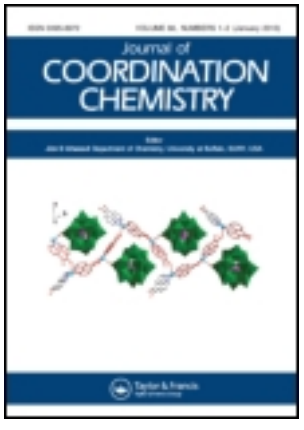

Journal of Coordination Chemistry
Publication details, including instructions for authors and subscription information:
http://www.tandfonline.com/loi/gcoo20

Ruthenium(II) ethylenediamine complexes with dipyridophenazine ligands: synthesis, characterization, DNA interactions, and antiproliferative activities

Mynam Shilpa [a], C. Shobha Devi [a], Penumaka Nagababu [a], J. Naveena Lavanya Latha [b], Ramjee Pallela [c], Venkateshwara Rao Janapala [c], K. Aravind [a] & S. Satyanarayana [a]

[a] Department of Chemistry, Osmania University, Hyderabad, India

[b] Department of Biotechnology, Krishna University, Machilipatnam, India

[c] Toxicology Unit, Biology Division, Indian Institute of Chemical Technology, Hyderabad, India

Accepted author version posted online: 22 Mar 2013.Published online: 29 Apr 2013.

To cite this article: Mynam Shilpa, C. Shobha Devi, Penumaka Nagababu, J. Naveena Lavanya Latha, Ramjee Pallela, Venkateshwara Rao Janapala, K. Aravind & S. Satyanarayana (2013) Ruthenium(II) ethylenediamine complexes with dipyridophenazine ligands: synthesis, characterization, DNA interactions, and antiproliferative activities, Journal of Coordination Chemistry, 66:10, 1661-1675, DOI: 10.1080/00958972.2013.788154

To link to this article: http://dx.doi.org/10.1080/00958972.2013.788154

Journal of Coordination Chemistry, 2013
Vol. 66, No. 10, 1661–1675, http://dx.doi.org/10.1080/00958972.2013.788154

Ruthenium(II) ethylenediamine complexes with dipyridophenazine ligands: synthesis, characterization, DNA interactions, and antiproliferative activities

MYNAM SHILPA†, C. SHOBHA DEVI†, PENUMAKA NAGABABU†, J. NAVEENA LAVANYA LATHA‡, RAMJEE PALLELA§, VENKATESHWARA RAO JANAPALA§, K. ARAVIND† and S. SATYANARAYANA†*

†Department of Chemistry, Osmania University, Hyderabad, India
‡Department of Biotechnology, Krishna University, Machilipatnam, India
§Toxicology Unit, Biology Division, Indian Institute of Chemical Technology, Hyderabad, India

(*Received 9 October 2012; in final form 30 January 2013*)

Ruthenium(II) complexes, $[Ru(en)_2dppz]^{2+}$ (**1**), $[Ru(en)_2qdppz]^{2+}$ (**2**), $[Ru(en)_2acdppz]^{2+}$ (**3**), and $[Ru(en)_2actatp]^{2+}$ (**4**), have been synthesized and characterized by IR, ^1H, ^{13}C-NMR and LC–MS. The interactions of these complexes with calf thymus (CT) DNA have been investigated by absorption, emission, viscosity, thermal denaturation, and circular dichroism. These techniques reveal that the complexes bind strongly to DNA. The apparent binding constants for the complexes decrease from **1** to **4** and are in the order of $8.5 \pm 0.2 \times 10^5$ M^{-1} (**1**), $7.3 \pm 0.8 \times 10^5$ M^{-1} (**2**), $4.3 \pm 0.3 \times 10^5$ M^{-1} (**3**), and $7.5 \pm 0.5 \times 10^4$ M^{-1} (**4**). The plot of log K versus log $[Na^+]$ yield slopes of -1.47, -1.44, -1.36, and -1.24 for **1**, **2**, **3,** and **4**, respectively. These complexes promote the photocleavage of pBR322 DNA. Cytotoxicities of these complexes suggest their possible anticancer activity.

Keywords: Ruthenium(II) complexes; DNA-Binding; Photocleavage; Anticancer activity

1. Introduction

Ruthenium(II) polypyridyl complexes have received attention as DNA-binding substrates due to rich photochemical and photophysical properties [1]. In two decades of research on the excited-state properties of ruthenium complexes [2], a variety of substituted 2,2′-bipyridine and 1,10-phenanthroline systems as well as other α,α′-diimine systems have been investigated as ligands for ruthenium(II) complexes. There has been considerable interest in DNA-binding properties of transition metal complexes [3–5].

Ruthenium polypyridyl complexes are promising DNA probes due to their intense MLCT luminescence, excited-state redox properties, and DNA-binding properties [6]. When such binding is through intercalation, complexes can be quite useful. Many studies have focused on the interaction of ruthenium complexes containing planar ligands which

*Corresponding author. Email: ssnsirasani@gmail.com

have good biological activities [7–10]. Most of the well-known platinum anticancer complexes have amines as ligands [11]. Inventions [12] of platinum-diamine complexes with excellent antitumor activity and lower renal toxicity than cisplatin have been reported. These studies suggest that at least one ligand must be a N-donor and should possess one hydrogen. Ruthenium(II) ethylenediamine complexes have similar DNA-binding properties to complexes containing phen or bpy as co-ligands [13], hence we concentrate on ethylenediamine co-ligands. In our earlier study, we have reported that several transition metal complexes containing ethylenediamine as co-ligands have good DNA-binding properties and cytotoxicities [14].

We have synthesized more $[Ru(en)_2L]^{2+}$ complexes (where en = ethylenediamine, **L** = dppz (**1**), qdppz (**2**), acdppz (**3**), and actatp (**4**) (figure 1)). Their synthesis, characterization, and DNA-binding properties are analyzed by absorption, emission, viscosity, thermal denaturation, circular dichroism, photosensitizing properties, and the anticancer studies were performed by MTT assay.

2. Experimental

2.1. *Materials and chemicals*

1,10-Phenanthroline-5,6-dione [15], daa = [9-(3,4-diaminophenyl)acridine] [16], dppz, qdppz, acdppz, and actatp [17, 18] were synthesized according to literature procedures. Doubly distilled water was used to prepare buffers. All chemicals were reagent grade. The

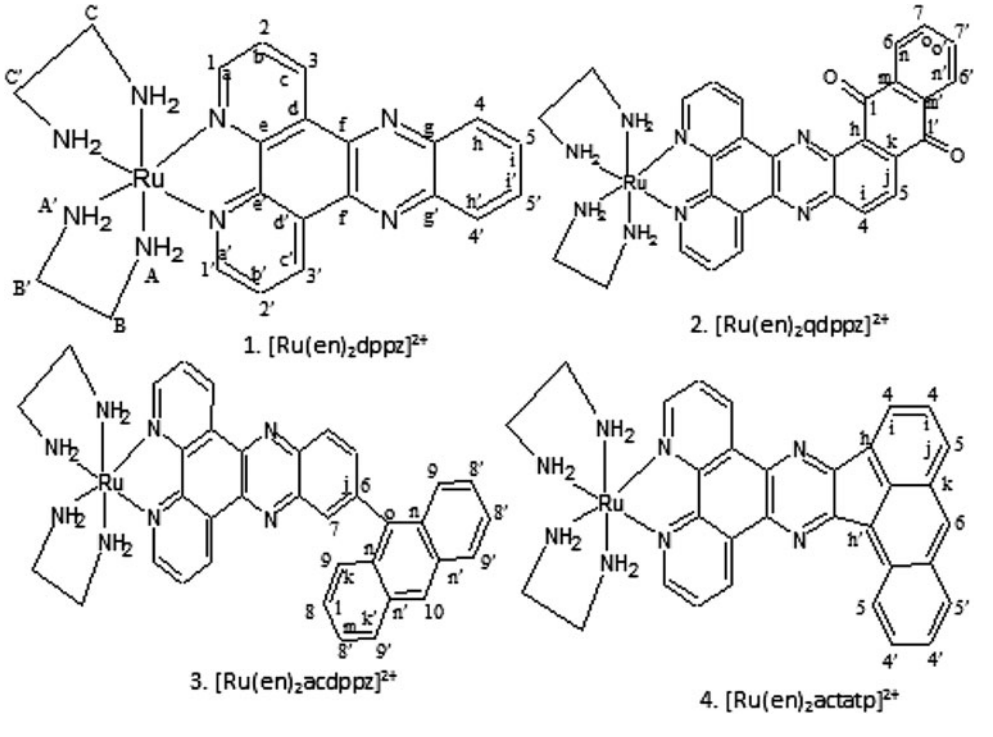

Figure 1. Molecular structures of **1**–**4**.

DNA concentration per nucleotide was determined by using a molar absorption coefficient ($6600\,M^{-1}\,cm^{-1}$) at 260 nm [19]. A ratio of 1.8–1.9 UV absorbance at 260 and 280 nm indicates that the DNA was sufficiently free of protein [20].

2.2. *Physical measurements*

IR spectra were recorded in KBr on a *Perkin-Elmer FT-IR-1605*. ^{1}H and ^{13}C-NMR spectra were measured on a *Varian XL-400 MHz* spectrometer with DMSO-d_6 as solvent at room temperature and tetramethylsilane (TMS) as the internal standard. LC–MS were recorded on a *2010A LQC system (Finnigan MAT)* with MeCN as mobile phase. UV–Visible spectra were recorded on an *Elico Bio-spectrophotometer model BL198*. Emission spectra were carried out by using an *Elico Bio-spectrofluorimeter model SL174* at room temperature. Circular dichroism spectra were recorded on a *JASCO J-810 spectropolarimeter*. Viscosity experiments were carried out in an *Ostwald viscometer* maintained at $30.0 \pm 0.1\,^{\circ}C$ in a thermostatic water bath.

2.3. *DNA-binding studies*

2.3.1. Emission studies. In emission studies, fixed metal complex concentrations (10 μM) were used and varying concentration (0–150 μM) of DNA was added. The excitation wavelength was fixed, and the emission range was adjusted before measurements. The fraction of ligand bound was calculated from the relation $C_b = C_t[(F - F_0)/F_{max} - F_0)]$, where C_t is the total complex concentration, F is the observed fluorescence emission intensity at a given DNA concentration, F_0 is the intensity in the absence of DNA, and F_{max} is when the complex is fully bound to DNA. Binding constant of fluorescence was obtained from a modified Scatchard equation using a plot of r/C_f *versus* r, where r is C_b/[DNA] and C_f is the concentration of the free complex. Fluorescence quenching was carried out by addition of 0.05 M of $[Fe(CN)_6]^{4-}$ and 1.0 M of KI as quencher to the complex in the presence and absence of DNA. According to the classical Stern–Volmer equation [21]

$$I_0/I = 1 + K_{sv}[Q]$$

where I_0 and I are the luminescence intensities in the absence and presence of quencher $[Fe(CN)_6]^{4-}$ or KI, respectively. K is a linear Stern–Volmer quenching constant depending on the ratio of the bound concentration of the complex to the concentration of DNA. [Q] is the concentration of the quencher $[Fe(CN)_6]^{4-}$ or KI.

2.3.2. Electronic absorption titration. Absorption titrations were carried out at room temperature to determine the binding affinity between DNA and the complex. A complex solution of 3.0 mL (20 μM) in a cuvette was placed in the sample compartment and then spectrum was recorded from 200 to 700 nm. During the titration, small aliquots (10 μL) of DNA solution were added to each cuvette (reference and sample) to eliminate the absorbance of DNA itself, and the solutions were mixed for ~5 min, then the absorption spectra were recorded. The titration process was repeated until there was no change in the spectra (binding saturation achieved). The changes in the metal complex concentration due to

dilution at the end of each titration were negligible. The intrinsic binding constant K_b was calculated from [22]

$$[DNA]/(\varepsilon_a - \varepsilon_f) = [DNA]/(\varepsilon_b - \varepsilon_f) + 1/(K_b(\varepsilon_b - \varepsilon_f))$$

where [DNA] is the concentration of DNA, ε_a, ε_f, and ε_b correspond to the extinction coefficient for the free metal complex, complex in the presence of DNA, and complex in fully bound form, respectively. In plots of $[DNA]/(\varepsilon_a - \varepsilon_f)$ *vs* [DNA], K_b is given by the ratio of slope to intercept.

2.4. *Viscosity experiments*

Viscosity experiments were carried out in an Ostwald viscometer maintained at 30.0 ± 0.1 °C in a thermostatic water bath. CT-DNA samples with approximately 200 base pairs were prepared by sonicating to minimize complexities arising from DNA flexibility [23]. Flow time was measured with a digital stop watch, each sample was measured three times, and an average flow time was calculated. Data were presented as $(\eta/\eta_0)^{1/3}$ *versus* [complex]/[DNA], where η is the viscosity of DNA in the presence of complexes and η_0 is the viscosity of DNA alone. Viscosity values were calculated from the observed flow time of DNA and DNA containing complex [24]

$$\eta_0 = t - t_0/t_0 \text{ and } \eta = t^1 - t_0/t_0$$

2.5. *Thermal denaturation studies*

Thermal denaturation studies were carried out with an *Elico Bio-spectrophotometer model BL198* by monitoring the absorbance at 260 nm with complex (10 μM) and CT-DNA (100 μM) [25]. Salt dependence studies were performed in tris buffer by titrating pre-formed complex-DNA adduct with various NaCl concentrations as indicated.

2.6. *DNA photocleavage experiment*

Photocleavage studies were carried out in a total volume of 10 μL containing pBR322 DNA (0.1 μg), and different concentrations of ruthenium(II) complexes were incubated for 30 min in the dark and then irradiated at room temperature with a UV lamp 365 nm for 60 min. Samples were analyzed by electrophoresis for 2.5 h at 40 V on a 0.8% agarose gel in buffer (pH 8.2). The gel was stained with 1 μg/mL ethidium bromide and then photographed under UV light.

2.7. *Circular dichroism*

Circular dichroism spectra of DNA were obtained by using a *JASCO J-810 spectropolarimeter* operating at 25 °C with 3 cm^3 of CT-DNA (90 μM dm^{-3}) sealed in a dialysis bag and 6 cm^3 of the complex (30 μM dm^{-3}) outside the bag and the system agitated on a shaker bath for 24 h. The region between 210 and 350 nm was scanned for each sample. Molecular ellipticity values were calculated according to the formula

$$[\theta]_\lambda = [\theta_\lambda/\mathrm{Cl}] \times 100$$

where $[\theta]_\lambda$ is the molecular ellipticity value at a particular wavelength expressed in degrees cm^2M^{-1}, C is the concentration of nucleotide phosphates per liter, l is the length of the cell in cm, and θ_λ is observed rotation in degrees.

2.8. *In-vitro cytotoxicity studies*

The cell line HL-60 (human myeloid leukemia) was obtained from the National Center for Cellular Sciences (NCCS), Pune, India. HL-60 cells were cultured in RPMI 1640 media supplemented with 10% (v/v) heat-inactivated fetal bovine serum (FBS), 100 units/mL penicillin and 100 μg/mL streptomycin. HL-60 cell lines were maintained in culture at 37 °C in an atmosphere of 5% CO_2. Cells were seeded in each well containing 100 μL medium at a final density of 2×10^4 cells/well, in 96-well micro titer plates at identical conditions. After overnight incubation, the cells were treated with different concentrations of testing complexes (20-100 μg/mL in RPMI 1640 medium and filtered) in a final volume of 200 μL with five replicates each. After 24 h, 10 μL of MTT [3-(4,5-dimethylthiazol-2-yl)-2,5-diphenyl tetrasolium bromide] (5 mg/mL) was added to each well and the plate was incubated at 37 °C in the dark for 4 h. The formazan crystals were solubilized in DMSO (100 μL/well), and the reduction in MTT was quantified by absorbance at 570 nm in a spectrophotometer (Spectra MAX Plus; Molecular Devices; supported by SOFT max PRO 3.0). Effects of test complexes on cell viability were calculated using untreated cells as the control. The data were subjected to linear regression analysis, and the regression lines were plotted for the best straight-line fit. The IC_{50} (50% inhibition of cell viability) concentrations were calculated using the respective regression equation.

2.9. *Synthesis of complexes*

2.9.1. $[Ru(en)_2dppz]^{2+}\cdot H_2O$ (1). This complex was prepared according to the method given in the literature [26]. A mixture of *cis*-$[Ru(en)_2Cl_2]Cl$ (0.074 g, 0.25 mM) and dppz (0.070 g, 0.25 mM) were placed in a 100 mL round-bottom flask containing 20 mL of methanol and refluxed for 2 h. The resulting brownish-red solution was allowed to cool at room temperature, and then, $NaClO_4$ in methanol was added. The thick crystalline precipitate of $[Ru(en)_2dppz]^{2+}$ that formed was collected and recrystallized from acetone/water. Yield: 70%. Analytical data: Elemental analysis (Expt. and Calcd for $C_{22}H_{28}N_8O_9Cl_2Ru$: Calcd (%): C, 52.47; H, 5.20; N, 22.25. Found (%): C, 52.15; H, 5.13; N, 22.14. IR (KBr, cm^{-1}): 1560 (C=N), 1450 (C=C), 616 (M – L), 473 (M – N (en)). LC–MS: 720 (found 721). ^{1}H-NMR (400 MHz, DMSO-d_6, TMS, δ): 9.2 (d, 2H, H_1, 1′), 9.10 (d, 2H, H_4, 4′), 8.4 (d, 2H, H_3, 3′), 8.2 (d, 2H, H_5, 5′), 6.6 (d, 2H, H_2, 2′), 3.22 (s, 4H, A, A′) and 2.87 (m, 4H, B, B′). ^{13}C[^{1}H]-NMR (100 MHz, DMSO-d_6, δ): 166.26 (2C, a, a′), 141.18 (2C, f, f′), 136.02 (2C, g, g′), 134.9 (2C, c, c′), 130.2 (4C, d, d′, h, h′), 129.4 (2C, e, e′), 127.4 (2C, b, b′), 52.64 (2C, C), 27.5 (2C, C′).

2.9.2. $[Ru(en)_2qdppz]^{2+}\cdot H_2O$ (2). *cis*-$[Ru(en)_2qdppz]^{2+}$ was prepared as above by replacing dppz with qdppz. The mixture was refluxed for 5 h with recrystallization from

acetone/water. Yield: 50%. Analytical data: Elemental analysis (Expt. and Calcd for $C_{30}H_{30}N_8O_{11}C_{l2}Ru$) Calcd (%): C, 56.86; H, 4.45; N, 17.68. Found (%): C, 56.35; H, 4.29; N, 17.42. IR (KBr, cm^{-1}): 1640 (C=O), 1540 (C=N), 1496 (C=C), 636 (M – L), 490 (M – N (en)). LC–MS: 852 (found 851). ^{1}H-NMR (DMSO-d_6, TMS, δ): 9.01 (d, 2H, H_1, 1′), 8.2 (d, 2H, H_4, 4′), 7.95 (d, 1H, H_5), 7.81 (d, 2H, H_3, 3′), 7.5 (d, 2H, H_6, 6′), 7.4 (s, 2H, H_7, 7′), 6.5 (d, 2H, H_2, 2′), 3.64 (s, 4H, A, A′), and 2.85 (m, 4H, B, B′). ^{13}C[^{1}H]-NMR (100 MHz, DMSO-d_6, δ): 175 (2C, l, l′), 159 (4C, a, a′, f, f′), 140 (6C, m, m′, g, g′, i, k), 132 (5C, c, c′, h, o, o′), 126.9 (6C, n, n′, d, d′, e, e′), 125.3 (3C, b, b′, j), 58.32 (2C, C), 27.4 (2C, C″).

2.9.3. [Ru(en)$_2$acdppz]$^{2+}$·H$_2$O (3). This complex was prepared as above by replacing dppz with acdppz. The mixture was refluxed for 8 h and recrystallized from 20 mL of water. Yield: 55%. Analytical data: Elemental analysis (Expt. and Calcd for $C_{35}H_{35}N_9O_9C_{l2}Ru$: Calcd (%): C, 61.75; H, 4.89; N, 18.52. Found (%): C, 61.53; H, 4.56; N, 18.69. IR (KBr, cm^{-1}): 1546 (C=N), 1460 (C=C), 679 (M – L), 491 (M – N (en)). LC–MS: 899 (found 890). ^{1}H-NMR (DMSO-d_6, TMS, δ): 8.23 (d, 2H, H_1, 1′), 8.22 (s, 1H, H_4), 7.95 (d, 2H, H_3, 3′), 7.70 (d, 4H, H_9, 9′), 7.62 (s, 1H, H_6), 7.56 (s, 1H, H_7), 7.54 (t, 4H, H_8, 8′), 7.35 (s, 1H, H_5), 7.20 (s, 1H, H_{10}), 7.15 (t, 2H, H_2, 2′), 2.6 (s, 4H, A, A′), and 2.2 (m, 4H, B, B′). ^{13}C[^{1}H]-NMR (100 MHz, DMSO-d_6, δ): 149.9 (6C, a, a′, f, f′ g, g′), 147.8 (6C, n, n′, o, i), 132.3 (3C, c, c′, j), 124.5 (5C, k, k′, h, e, e′), 123.4 (4C, l, l′, d, d′, e, e′), 123.16 (8C, b, b′, k, k′, m, m′), 65.48 (2C, C), 29.5 (2C, C′).

2.9.4. [Ru(en)$_2$actatp]$^{2+}$H$_2$O (4). [Ru(en)$_2$actatp]$^{2+}$ was prepared as above by replacing dppz with actatp. The mixture was refluxed for 8 h and recrystallized from 20 mL of water. Yield: 40%. Analytical data: Elemental analysis (Expt. and Calcd for $C_{32}H_{32}N_8O_9C_{l2}Ru$: Calcd (%): C, 61.23; H, 4.82; N, 17.85. Found (%): C, 61.12; H, 4.56; N, 17.56. IR (KBr, cm^{-1}): 1565 (C=N), 1430 (C=C), 605 (M – L), 497 (M – N (en)). LC–MS: 847 (found 845). ^{1}H-NMR (DMSO-d_6, TMS, δ): 9.13 (d, 2H, H_1, 1′), 9.08 (s, 1H, H_7), 8.37 (d, 2H, H_3, 3′), 7.9 (d, 2H, H_6, 6′), 7.5 (m, 4H, H_4, 4′, H_5, 5′), 7.24 (t, 2H, H_2, 2′), 2.9 (s, 4H, A, A′), and 2.4 (m, 4H, B, B′). ^{13}C[^{1}H]-NMR (100 MHz, DMSO-d_6, δ): 138.3 (2C, a, a′), 137.5 (4C, f, f′, g, g′), 135.6 (2C, c, c′), 133.4 (4C, k, k′), 132.1 (5C, j, j′, d, d′), 131.4 (4C, h, h′, e, e′), 129.8 (4C, i, i′), 126.3 (2C, b, b′), 68.22 (2C, C), 30.2 (2C, C′).

3. Results and discussion

3.1. *Emission studies*

In the absence of DNA, the complexes upon excitation at 457, 468, 420, and 468 nm have emission at 610, 536, 540, 520 nm for **1**, **2**, **3,** and **4**. Upon addition of CT-DNA, the emission intensities of the complexes increase by 2.35, 2.12, 1.68, and 1.53 for **1**, **2**, **3,** and **4** (figure 2). This implies that the complexes strongly interact with DNA and are protected by DNA, since the hydrophobic environment inside the DNA helix reduces the accessibility of water and the complexes mobility is restricted at the binding site, leading to decrease in the vibrational modes of relaxation and hence fluorescence intensity

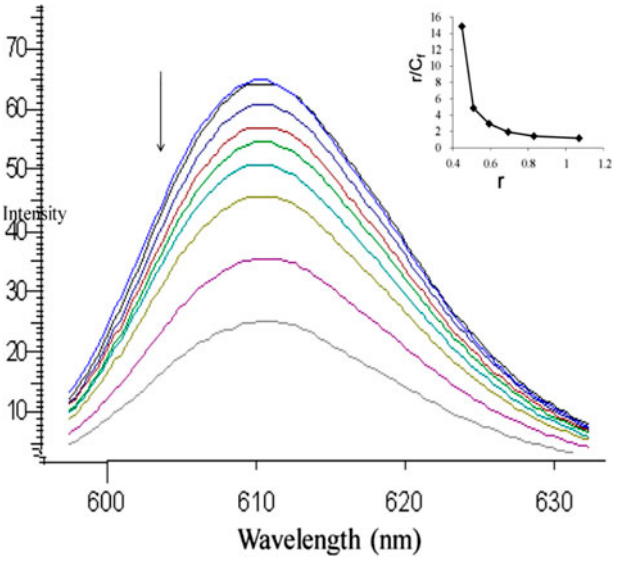

Figure 2. Fluorescence emission spectra of $[Ru(en)_2dppz]^{2+}$ in tris buffer in the presence of CT DNA, [Ru] = 10 µL (3×10^{-6}), [DNA] = 0–150 µM. λ_{exc} = 457 nm, λ_{emi} = 610 nm. The insert shows the best fit of data to r/C_f *vs. r*.

increases. Fluorescence binding constant calculated for all complexes are $8.9 \pm 0.5 \times 10^5$ M^{-1} (**1**), $7.6 \pm 0.8 \times 10^5$ M^{-1} (**2**), $5.2 \pm 0.2 \times 10^5$ M^{-1} (**3**), and $8.2 \pm 0.4 \times 10^4$ M^{-1} (**4**). This observation is further supported by fluorescence quenching experiments using $[Fe(CN)_6]^{4-}$ (0.1 M) and KI (1 M) as quenchers. In the plot of I_0/I *versus* [*Q*], the slope is the K_{sv}. K_{sv} values are smaller in the presence of DNA as complexes bound to DNA can be protected from the quencher, because highly negatively charged $[Fe(CN)_6]^{4-}$ would be repelled by the negative DNA phosphate backbone, hindering quenching of the emission of the bound complex [27], hence quenching is small. At higher concentration of DNA, the slope is almost zero, indicating that the bound species is inaccessible to quencher. Comparing with ferrocyanide, KI shows less quenching affinity, because KI is mononegative, whereas ferrocyanide is tetra negative. Ferrocyanide quenching and KI fluorescence quenching curves of complexes when bound to DNA are given in figure 3 and K_{sv} values are given in table 1. From absorption and fluorescence spectroscopy, the binding of complexes with DNA is in the order **1** > **2** > **3** > **4**.

3.2. *Absorption studies*

DNA-binding studies can be conveniently monitored by absorption spectroscopy [28]. The electronic absorption spectra of complexes in the presence of increasing amount of DNA in tris buffer are shown in figure 4. In the UV region, intense absorptions at 346 nm for $[Ru(en)_2dppz]^{2+}$, 318 nm for $[Ru(en)_2qdppz]^{2+}$, 305 nm for $[Ru(en)_2acdppz]^{2+}$, and 312 nm for $[Ru(en)_2actatp]^{2+}$ were attributed to intra ligand π–π^* transition of the complexes. The broad MLCT absorptions at 466, 463, 445, and 463 nm for **1**, **2**, **3,** and **4**, respectively, attributed to Ru(dπ)→*L*–*L*(π^*) transitions of the complex were significantly perturbed, indicating interaction of complex with DNA. This band is bathochromically shifted relative to

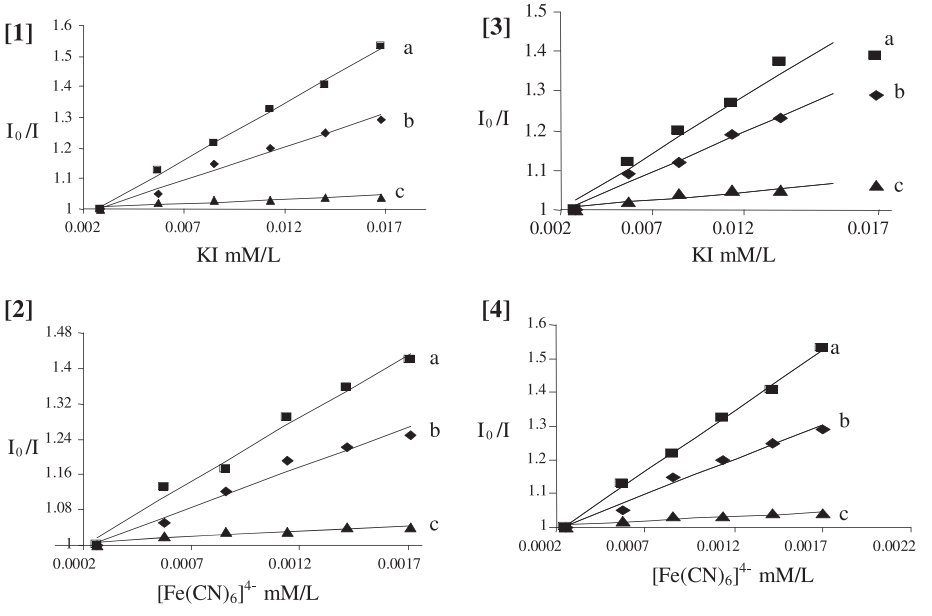

Figure 3. Emission quenching curves of **1**, **3** with KI and **2**, **4** with $[Fe(CN)_6]^{4-}$ in absence of DNA (a), presence of DNA 1:50 (b) and 1:200 (c).

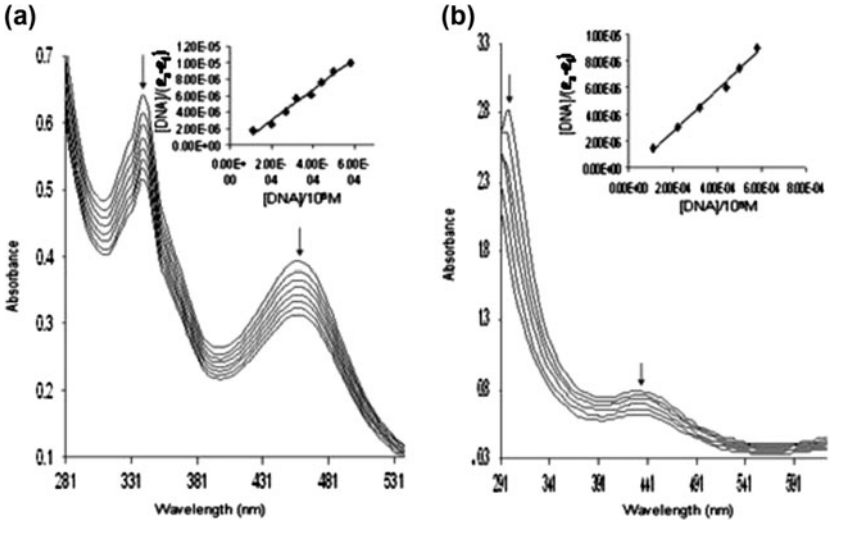

Figure 4. Absorption spectra of $[Ru(en)_2dppz]^{2+}$ (**a**) and $[Ru(en)_2qdppz]^{2+}$ (**b**) in tris buffer upon addition of CT DNA in absence (top) and presence of CT DNA (lower), [Ru] = 10 μM; [DNA] = 0–126 μM. Insert: plots of $[DNA]/(\varepsilon_a-\varepsilon_f)$ *vs.* [DNA] for the titration of DNA with complex. Solid line is linear fitting of the data. Arrow shows change in absorption with increasing DNA concentration.

those of $[Ru(phen)_3]^{2+}$ (448 nm) [29], in accord with extension of the framework. Upon increasing the CT-DNA concentration, hypochromism was 13% with a red shift of 6 nm

for $[Ru(en)_2dppz]^{2+}$, 10% with a red shift of 5 nm for $[Ru(en)_2qdppz]^{2+}$, 7.6% with a red shift of 3 nm for $[Ru(en)_2acdppz]^{2+}$, and 7% with a red shift of 3 nm for $[Ru(en)_2actatp]^{2+}$. Since the ligand intercalates into the base pairs of DNA, the π^* orbital of the intercalating ligand can couple with the π orbital of the base pairs; the coupling π^* orbital is partially filled by electrons, thus decreasing the transition probabilities, resulting in hypochromism. These data imply that these complexes bind to DNA in an intercalative mode [30].

In order to further investigate the binding strength of the complexes, the intrinsic binding constants K_b of the complexes with CT-DNA were calculated as $8.5 \pm 0.2 \times 10^5$ M^{-1} (**1**), $7.33 \pm 0.8 \times 10^5$ M^{-1} (**2**), $4.3 \pm 0.3 \times 10^5$ M^{-1} (**3**), and $7.5 \pm 0.5 \times 10^4$ M^{-1} (**4**); these values were slightly higher than those obtained by the emission titration method. The difference between K_b values obtained by absorption and fluorescence techniques is in agreement with earlier reports [31]. The binding constants of these complexes are smaller when compared to the similar complexes with different ancillary ligands, in the range of 105–106 M^{-1} [32]; comparing with ethylenediamine, bpy and phen are aromatic and more planar. Among these four intercalating ligands, dppz is more planar than the other ligands. The binding constant data confirm that **1** > **2** > **3** > **4** as the order and all bind strongly to CT-DNA.

Generally, the intercalative ligand should contain an aromatic heterocyclic functionality such as dppz (extended basic ligands) and imidazole (extended planar ligands) that can insert and stack between the base pairs of double helical DNA. Extension of intercalative ligand increases the strength of interaction and binding constant of the complex with DNA [9, 33].

Since an octahedral complex binds to DNA in three dimensions, its ancillary ligand can also be modified or functionalized to tune the DNA binding; if the ancillary ligand is bulky with nonaromatic groups such as $-CH_3$, the DNA binding of the complex will be weakened. The ancillary ligand phen expands the π-delocalization and thus decreases the sigma donor capacity of the metal ion, leading to a decrease in the electron density on the metal ion and in turn stabilization of metal dπ orbital but destabilization of the ligand π^* orbital [34]. Additionally, the increased hydrophobicity of the complexes leads to self-stacking in solution, and this effect may reduce the net binding affinity. The binding constants of the complexes follow the trend of $[Ru(ip)_2dppz]^{2+}$ $(2.1 \times 10^7\,M^{-1}) > [Ru(phen)_2dppz]^{2+}$ $(7.5 \times 10^6\ M^{-1}) > [Ru(bpy)_2dppz]^{2+}$ $(4.9 \times 10^5\,M^{-1}) > [Ru(en)_2dppz]^{2+}$ $(8.5 \times 10^5\,M^{-1})$. This may be explained by the planar area of the ancillary ligand ip is larger than that of the phen, bpy, and en. In contrast, $[Ru(phen)_3]^{2+}$ and $[Ru(dip)_3]^{2+}$ show strong affinity for DNA, following the order en < bpy < phen ⩽ dip < ip [13, 14, 35].

3.3. *Viscosity measurements*

To further clarify the interactions between complexes and DNA, viscosity measurements were carried out. Hydrodynamic measurements which are sensitive to length increases (i.e. viscosity, sedimentation) are regarded as the least ambiguous and the most critical tests of binding model in solution in the absence of crystallographic structural data [36]. Intercalation results in lengthening the DNA helix, as base pairs are separated to accommodate the binding ligand, leading to increase in DNA viscosity. Figure 5 shows the effects of **1**, **2**, **3,** and **4** and ethidium bromide on the viscosity of rod-like DNA. Ethidium bromide is a known DNA classical intercalator and increases the relative specific viscosity by lengthening of the DNA double helix through intercalation. Upon increasing the amount of complex, the relative viscosity of DNA increases steadily, similar to the behavior of

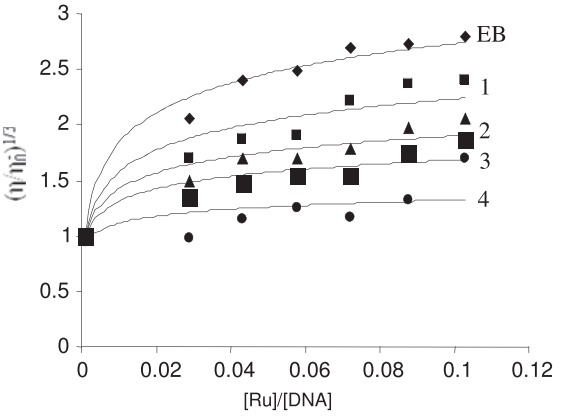

Figure 5. Effect of increasing amounts of ethidium bromide (EB), **1**, **2**, **3** and **4** on the relative viscosity of CT-DNA at 25 (±0.1) °C. [DNA] = 0.5 mM.

ethidium bromide. The increased degree of viscosity may depend on the intercalative affinity for DNA and follows the order **EB** > **1** > **2** > **3** > **4**.

3.4. *Thermal denaturation studies*

The melting of DNA is an important parameter to study the interaction of transition metal complexes with nucleic acids. Thermal denaturation of DNA in the presence of complexes can give insight into their conformational changes when temperature is raised and offer information about the interaction strength of complexes with DNA. The melting temperature T_m, at which 50% of the DNA has become single strand, can be determined from the thermal denaturation curves of DNA by monitoring absorption changes at 260 nm. According to the literature [37], the intercalation of natural or synthesized organics and metallointercalators generally results in considerable increase in melting temperature (T_m). DNA melting revealed that T_m of CT-DNA was 60 °C and T_m in the presence of **1**, **2**, **3,** and **4** (20 μM) are 71 ± 0.1, 69 ± 0.1, 66 ± 0.1, and 65 ± 0.1 °C, respectively, under our experimental conditions. The observed melting temperature in the presence of complexes reveals strong classical intercalation [38] and shows that interaction of $[Ru(en)_2dppz]^{2+}$ with DNA is the strongest.

3.5. *Salt dependence studies*

The salt dependence binding of **1**, **2**, **3,** and **4** to DNA is shown in figure 6. As the concentration of NaCl increases, the binding constant decreases. The dependence of binding constant for these complexes upon Na^+ concentration is a consequence of the linkage of complex and Na^+ binding to DNA and may be analyzed by polyelectrolyte theory [39]. The slope of the lines in figure 6 provides an estimate of $Z\psi$, where ψ is the fraction of counter ions associated with each DNA phosphate ($\psi = 0.88$ for DNA) and Z is the charge on the complex ($Z = +2$). The slopes of the lines in figure 6 are −1.47, −1.44, −1.36, and −1.24 for **1**, **2**, **3,** and **4**, respectively. These values are less than the theoretically expected values of $Z\psi$ ($2 \times 0.88 = 1.76$). Such lower values could arise from coupled anion release

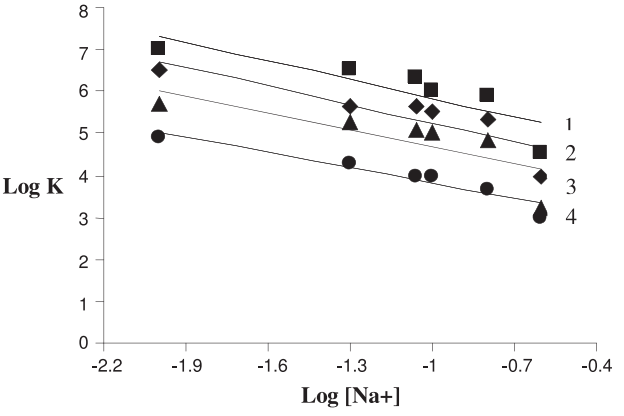

Figure 6. Salt dependence of the equilibrium binding constants for DNA binding of **1**, **2**, **3** and **4**. The lines indicate the slope of the linear square fit to the data as −1.47 (**1**), −1.44 (**2**), −1.36 (**3**) and −1.24 (**4**).

or from change in complex or DNA hydration upon binding. The knowledge of $Z\psi$ allows for a quantitative estimation of the nonelectrostatic contribution to the DNA binding constant for these complexes.

3.6. *Photoactivated cleavage of Ru(II) complexes*

There is substantial and continuing interest in DNA endonucleolytic cleavage activated by metal ions [40, 41]. Control runs in the agarose gel electrophoresis experiments suggest that untreated plasmid pBR322 DNA does not show cleavage. Complexes exhibit concentration-dependent, single-strand cleavage of supercoiled Form I to the nicked Form II DNA (figure 7). Upon increasing the concentration of complexes, the amount of Form II increases gradually, while Form I diminished gradually. This is the result of single-stranded cleavage of pBR322 DNA. That neither irradiation of DNA alone at 365 nm (without Ru (II)) nor incubation with Ru(II) without light yields significant strand scission indicates Ru (II) complexes play an important role in the DNA cleavage. To identify the nature of the

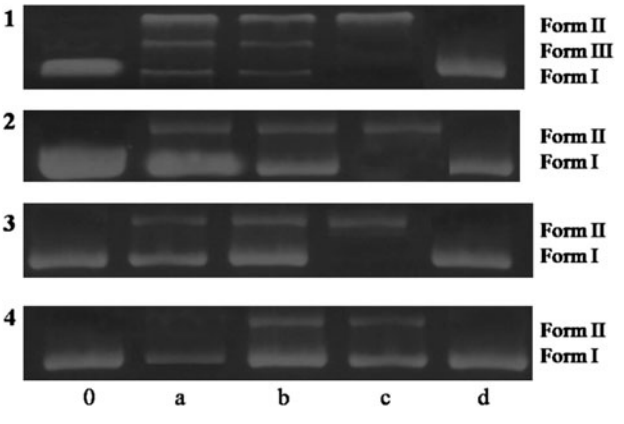

Figure 7. Photocleavage of pBR322 DNA in the absence and presence of **1**, **2**, **3** and **4** after 60 min irradiation at 365 nm. Lane 0 control plasmid DNA (untreated pBR322), lanes a to c addition of complexes, in amounts of 20, 30, 40 μM of concentration, and lane d complexes in presence of histidine (2 mM).

reactive species responsible for photoactivated cleavage of plasmid DNA, we have investigated with singlet oxygen inhibiting agent histidine. Figure 7 shows the photocleavage of pBR322 DNA in the presence of complex alone and complex + histidine. Indeed, plasmid DNA cleavage by **1–4** was inhibited in the presence of histidine (lane d).

3.7. *Circular dichroism*

Circular dichroism is useful in diagnosing changes in DNA morphology during drug-DNA interactions, as the band due to base stacking (+275 nm) and that due to right-handed helicity (−248 nm) are quite sensitive to the mode of DNA interactions with small molecules [42]. The changes in CD signals of DNA observed on interaction with drugs may be assigned to the corresponding changes in DNA structure [42]. Intercalation shows more perturbation on the base stacking and increasing of molecular ellipticity, whereas electrostatic interactions show less/no perturbation on the base stacking and decrease in molecular ellipticity. The CD spectrum of the complexes is shown in figure 8 and molecular ellipticity values are given in table 1 as **1** > **2** > **3** > **4**.

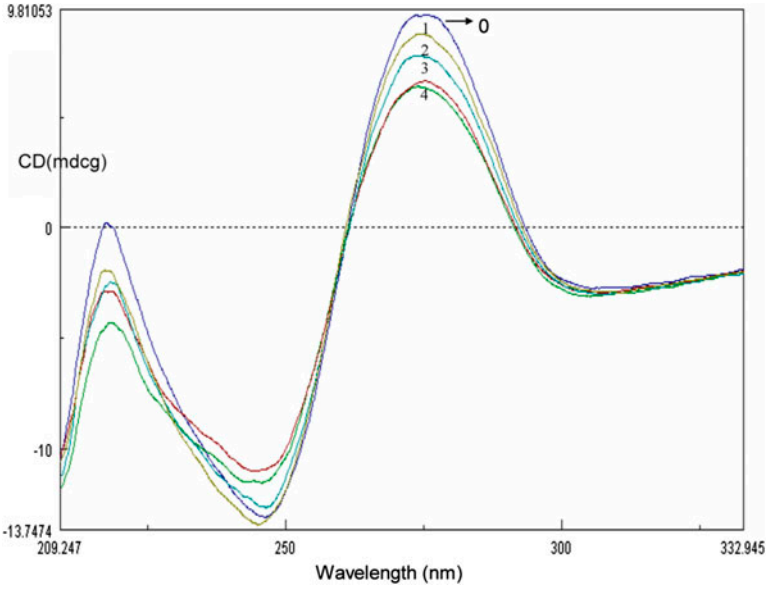

Figure 8. Circular dichroism spectra of CT-DNA in the absence (0) and presence of **1**, **2**, **3** and **4** after 24 h dialysis.

Table 1. Quenching constant (K_{sv}) data of complexes in the absence and presence of DNA (1 : 50, 1 : 200) with $[Fe(CN)_6]^{4-}$ and KI as quencher and molecular ellipticity values of complexes in the presence of DNA after 24 h dialysis.

	$[K_4(Fe(CN)_6]^{4-}$ (0.01 M)			KI (1 M)			
Complex	Only complex	1 : 50	1 : 200	Only complex	1 : 50	1 : 200	Molecular ellipticity
$[Ru(en)_2dppz]^{2+}$	3328	249.3	46.9	620	15.2	0.43	56,452
$[Ru(en)_2qdppz]^{2+}$	1023	371.5	58.2	580	20.6	0.57	52,753
$[Ru(en)_2acdppz]^{2+}$	875.3	334.2	85.3	452	35.2	1.27	48,256
$[Ru(en)_2actatp]^{2+}$	763.3	375.6	103	420	42.3	7.25	40,238

3.8. *Antiproliferative activity*

Cell proliferation or viability was measured using the MTT assay [43]. The cytotoxic effects of test complexes were investigated on human leukemia cell lines (HL-60). After 24 h of treatment, the number of live cells was measured by MTT assay and IC_{50} values for each testing complex were determined (table 2). It is evident from table 2 that HL-60 cells were moderately sensitive to **1**, with an IC_{50} value of 22.30 μg/mL, as compared with other complexes. Complex **2** did not show any activity against the HL-60 cells, and the decreasing order of activity among the test complexes was in the order **1** > **3** > **4**. DMSO stock solution was used for all complexes to perform a proper comparison among the complexes; untreated cells containing the same amount of DMSO are taken as negative controls. Cisplatin was used as the positive control. These complexes exhibited dose-dependent growth inhibitory effect (figure 9) against the tested cell lines. The structure of the mixed ligand complexes could be a factor for exhibiting differential anti-proliferative activities on the cancerous cell lines (figure 10). These results are in agreement with reported ruthenium polypyridyl complexes [7, 8].

Table 2. Cytotoxic activity of mixed ligand ruthenium(II) complexes on HL-60 cells.

Complexes	(IC_{50} values in μg/mL)	(IC_{50} values in μM)
1	21.30 ± 0.81	37.85 ± 1.62
2	No activity	No activity
3	25.72 ± 1.13	40.89 ± 1.55
4	56.59 ± 1.46	81.74 ± 1.26
Cisplatin	18.15 ± 1.16	21.12 ± 1.26

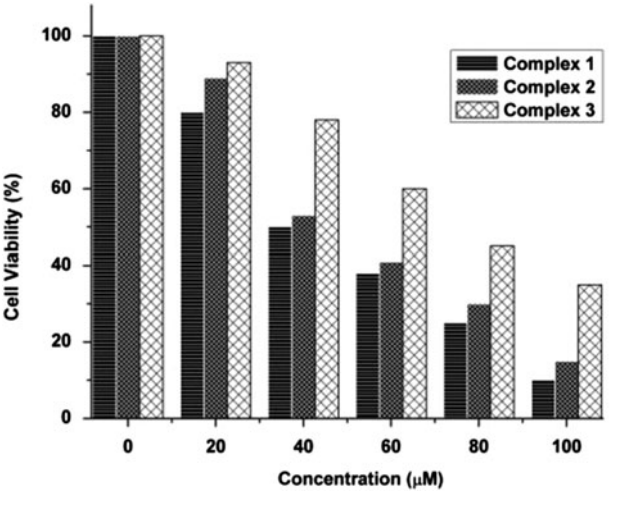

Figure 9. *In-vitro* cytotoxity of **1**, **3** and **4** on tumor cell line HL-60 after treatment of 24 h in the absence (control) and presence of different concentrations.

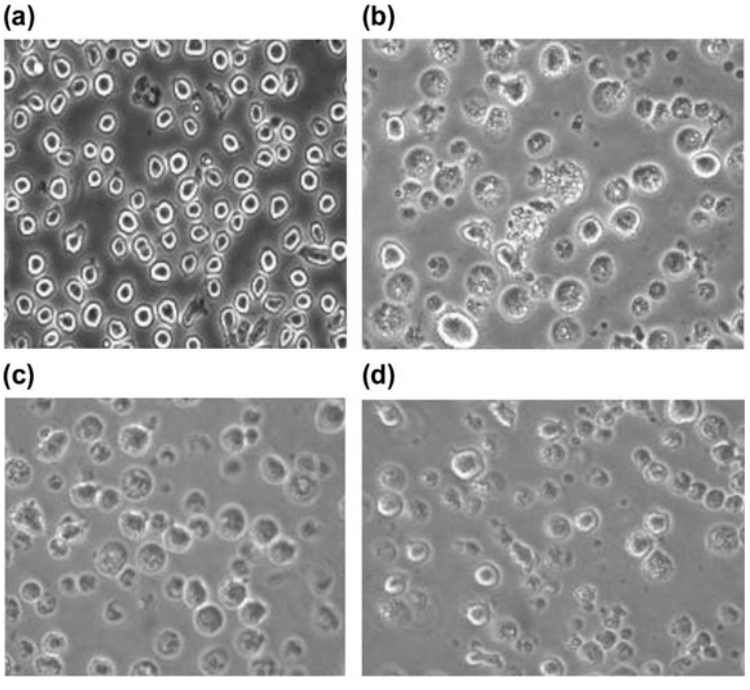

Figure 10. The morphological effects exerted by complexes on HL-60 cells 24 h after treatment. Photographs were taken using a Nikon inverted light microscope (20 × objective). a shows the untreated cells and b, c and d show cells treated with 0.5 mM of **1**, **3** and **4** complexes, respectively.

4. Conclusion

Four ethylenediammine Ru(II) complexes with extended planar aromatic ligands have been synthesized, characterized, and their interaction with CT-DNA examined. Absorption, emission, thermal denaturation, and viscosity experiments were performed and the results suggest an intercalative mode of DNA binding. The planarity of the modified dipyridophenazine plays an important role in dictating DNA-binding affinity. Thus, the dppz complex binds to DNA more strongly and follows the order qddpz > acdppz > actatp. The present study demonstrates that the ancillary ligands with hydrogen bonding potential support the intercalative interaction of ligands with extended aromatic rings and enhances the DNA-binding affinity. However, for ethylenediamine complexes with ligands like actatp, a decrease in binding affinity has been observed illustrating that minor changes in the ligand architecture and electronic structure can remarkably change the DNA-binding affinity. The results of the present study show that the complexes could be potential anticancer agents.

Acknowledgements

We are grateful to the DST (Department of Science and Technology) India for providing financial support and also thankful to Dr. Bhanuprakash (Scientist, NIN) for providing CD facilities.

References

[1] E.M. Boon, J.K. Barton. *Curr. Opin. Struct. Biol.*, **12**, 320 (2000).
[2] J.P. Paris, W.W. Brandt. *J. Am. Chem. Soc.*, **81**, 5001 (1959).
[3] B. Norden, P. Lincoln, B. Akerman, E. Tuite. *Met. Ions Biol. Syst.*, **33**, 177 (1996).
[4] K.E. Erkkila, D.T. Odom, J.K. Barton. *Chem. Rev.*, **99**, 2777 (1999).
[5] Y. Xiong, L.-N. Ji. *Coord. Chem. Rev.*, **185**, 711 (1999).
[6] C.V. Kumar, J.K. Barton, N.J. Turro. *J. Am. Chem. Soc.*, **107**, 5518 (1985).
[7] H.-L. Huang, Z.-Z. Li, Z.-H. Liang, J.H. Yao, Y.-J. Liu. *Eur. J. Med. Chem.*, **46**, 3282 (2011).
[8] H.-L. Huang, Z.-Z. Li, X.-Z. Wang, Z.-H. Liang, Y.-J. Liu. *J. Coord. Chem.*, **65**, 3287 (2012).
[9] X.-W. Liu, Y.-D. Chen, L. Li. *J. Coord. Chem.*, **65**, 3050 (2012).
[10] Y.-J. Liu, Z.-H. Liang, Z.-Z. Li, J.-H. Yao, H.-L. Huang. *J. Organomet. Chem.*, **696**, 2728 (2011).
[11] J.M. Perez, A.G. Quiroga, E.I. Montero, C. Alonso, C. Navarro-Ranninger. *J. Inorg. Biochem.*, **73**, 235 (1999).
[12] I. Kostova. *Recent Pat. Anti-Cancer Drug Discovery*, **1**, 1 (2006).
[13] P. Nagababu, M. Shilpa, M.B. Mustafa, P. Ramjee, S. Satyanarayana. *Inorg. React. Mech.*, **6**, 301 (2008).
[14] P. Nagababu, S. Satyanarayana. *Polyhedron*, **26**, 1686 (2007).
[15] M. Yamada, Y. Tanaka, Y. Yoshimato, S. Kuroda, I. Shimao. *J. Bull. Chem. Soc. Jpn.*, **65**, 1006 (1992).
[16] M.J. Plater, I. Greig, M.H. Helfrich, S.H. Ralston. *J. Chem. Soc. Perkin Trans.*, **1**, 2553 (2001).
[17] A. Ambroise, B.G. Maiya. *Inorg. Chem.*, **39**, 4256 (2000).
[18] H. Deng, H. Xu, Y. Yang, H. Li, H. Zou, L.-H. Qu, L.-N. Ji. *J. Inorg. Biochem.*, **97**, 207 (2003).
[19] M.E. Reichmann, S.A. Rice, C.A. Thomas, P. Doty. *J. Am. Chem. Soc.*, **76**, 3047 (1954).
[20] J. Marmur. *J. Mol. Biol.*, **3**, 208 (1961).
[21] J.R. Lakowicz, *Topics in Fluorescence Spectroscopy*, Vol. 1, p. 53, Plenum Press, New York, NY (1991).
[22] A. Wolfe, G.H. Shimer, T. Meehan. *Biochemistry*, **26**, 6392 (1987).
[23] J.B. Chaires, N. Dattagupta, D.M. Crothers. *Biochemistry*, **21**, 3927 (1982).
[24] S. Satyanarayana, J.C. Dabrowiak, J.B. Chaires. *Biochemistry*, **32**, 2573 (1993).
[25] E. Tselepi-Kalouli, N. Katsaros. *J. Inorg. Biochem.*, **37**, 271 (1989).
[26] B.P. Sullivan, D.J. Salmon, T.J. Meyer. *Inorg. Chem.*, **17**, 3334 (1978).
[27] C.V. Kumar, N.J. Turro, J.K. Barton. *J. Am. Chem. Soc.*, **107**, 9319 (1985).
[28] J.E.B. Johnson, R.R. Ruminski. *Inorg. Chim. Acta*, **208**, 231 (1993).
[29] J.-G. Liu, Q.-L. Zhang, L.-N. Ji, Y.-Y. Cao, X.-F. Shi. *Transition Met. Chem.*, **26**, 733 (2001).
[30] J.G. Liu, B.H. Ye, Q.L. Zhang, X.H. Zou, Q.X. Zhen, X. Tian, L.-N. Ji. *J. Bio. Inorg. Chem.*, **5**, 119 (1996).
[31] S. Murali, C.V. Sastri, B.G. Maiya. *Proc. Indian Acad. Sci. (Chem. Sci.)*, **114**, 403 (2002).
[32] Y. Praveen Kumar, M. Shilpa, P. Nagababu, M. Rajender Reddy, K.L. Reddy, N. Md Gabra, S. Satyanarayana. *J. Fluoresc.*, **3**, 835 (2012).
[33] C. Shobha Devi, S. Satyanarayana. *J. Coord. Chem.*, **65**, 474 (2012).
[34] T.K. Schock, J.L. Hubbard, C.R. Zoch, G.B. Yi, M. Sorlie. *Inorg. Chem.*, **22**, 1617 (1983).
[35] P. Nagababu, J.N. Lavanya Latha, S. Satyanarayana. *Chem. Biodivers.*, **3**, 1219 (2006).
[36] G.A. Neyhart, N. Grover, S.R. Smith, W.A. Kalsbeck, T.A. Fairly, M. Cory, H.H. Thorp. *J. Am. Chem. Soc.*, **115**, 4423 (1993).
[37] S. Satyanarayana, J.C. Dabrowiak, J.B. Chaires. *Biochemistry*, **31**, 9319 (1992).
[38] T. Takahashi, H. Tanaka, A. Matsuda, H. Yamada, T. Matsumoto, S. Yukio. *Tetrahedron Lett.*, **37**, 2433 (1996).
[39] M.T. Record, C.F. Anderson, T.M. Lohman. *Rev. Biophys.*, **11**, 103 (1978).
[40] R.P. Hertzberg, P.B. Dervan. *J. Am. Chem. Soc.*, **104**, 313 (1982).
[41] D.S. Sigman, D.R. Graham, L.E. Marshall, K.A. Reich. *J. Am. Chem. Soc.*, **102**, 5419 (1980).
[42] V.I. Ivanov, L.E. Minchenkova, A.K. Schyolkina, A.I. Poletayev. *Biopolymers*, **12**, 89 (1973).
[43] T. Mosmann. *J. Immunol. Methods*, **65**, 55 (1983).